JOURNAL OF BONE AND MINERAL RESEARCH
Volume 16, Number 8, 2001

Variability in Skeletal Mass, Structure, and Biomechanical Properties Among Inbred Strains of Rats

CHARLES H. TURNER,[1,2] RYAN K. ROEDER,[1] ARLO WIECZOREK,[1] TATIANA FOROUD,[3] GUANGDA LIU,[4] and MUNRO PEACOCK[4]

ABSTRACT

The aim of this study was to assess the usefulness of the inbred rat model for studies of genetic influences on skeletal fragility. We characterized bone mass, geometry, and skeletal biomechanics in 11 inbred strains of rats. This study showed that considerable variation exists in bone structure, areal bone mineral density (aBMD), and fragility phenotypes among inbred strains of rats. Interestingly, the variability in skeletal phenotypes in rats was site specific, suggesting that no single gene regulates skeletal fragility at all sites. For instance, the Copenhagen 2331 (COP) strain had the greatest biomechanical properties in the femoral neck but only modest bone strength at the femoral midshaft, compared with other strains. Consequently, COP rats appear to have alleles that specifically enhance femoral neck biomechanical properties and may serve as a model for studying genetic influences on hip strength. The Brown Norway (BN) and Fischer 344 (F344) strains may provide models for vertebral fragility because each has relatively fragile lumbar vertebrae. The F344 rats also had the most fragile femora and, thus, appear to carry alleles that cause overall skeletal fragility. We identified two inbred rat crosses that will facilitate the study of genetic influences on skeletal fragility at clinically relevant skeletal sites: Lewis (LEW) with F344 (primarily for vertebral fragility) and COP with DA (primarily for femoral neck fragility). The results strongly suggest that selected crosses of inbred strains of rats will provide useful models for studying genetic influences on bone strength and structure. (J Bone Miner Res 2001;16:1532–1539)

Key words: bone density, biomechanics, genetics, rat, bone strength

INTRODUCTION

PEAK BONE mineral density (BMD) is a highly heritable trait.[1–3] Although BMD is a major component determining the ability of bone to resist fracture, other traits such as bone geometry or structure and tissue quality also play important roles. Currently, the key genes that influence bone structure and strength have not been identified. Identification of the genes that underlie the components of bone strength will provide fundamental information and improve our understanding of the pathophysiology and treatment of osteoporotic fracture.

The use of animal models with relevant biological phenotypes related to disease models may provide important genetic clues that will improve the efficiency of identifying genes underlying bone strength. Well-characterized animal lines with phenotypes related to certain aspects of human osteoporosis can be used as an approach to study more homogeneous populations in which isolation of candidate chromosomal regions and genetic loci should be faster and

[1]Department of Orthopedic Surgery, Indiana University School of Medicine, Indianapolis, Indiana, USA.
[2]Department of Mechanical Engineering, Purdue School of Engineering and Technology, Indianapolis, Indiana, USA.
[3]Department of Medical and Molecular Genetics, Indiana University School of Medicine, Indianapolis, Indiana, USA.
[4]Department of Medicine, Indiana University School of Medicine, Indianapolis, Indiana, USA.

more efficient.[4] Animal models complement and extend human studies by allowing close control of environmental factors by expanding the characterization of phenotypes underlying bone strength and by facilitating breeding strategies to identify genetic linkage. Of particular value are experimental approaches using inbred animals. Although individuals within an inbred strain are genetically identical, genetic differences exist between different inbred strains. Where there are differences in bone fragility between two inbred strains, one can identify the genetic differences that are linked to the variation in bone fragility phenotypes.

Studies using the quantitative trait loci (QTL) approach with inbred strains of mice have provided some promising new information about the genetic influence on BMD.[5,6] Inbred rats are a potentially useful genetic model that is yet to be studied. The ovariectomized rat generally is accepted as an excellent animal model for studying postmenopausal bone loss.[7,8] Importantly, rats have been used extensively for biomechanical analyses of bone fragility and have served as a highly predictive model of fracture risk in humans.[9] Furthermore, considerable progress has already been made in mapping the rat genome.[10] Currently, there are thousands of simple sequence length polymorphism (SSLP) markers for rat genetics studies, making the investigation of genetic influences on skeletal phenotypes quite feasible.[11–13]

In this study, we characterized bone mass, geometry, and skeletal fragility in 11 inbred strains of rats. We hypothesized that there would be considerable variability among the strains in these phenotypes indicating that the genetic differences between the strains contribute to changes in bone fragility phenotype.

MATERIALS AND METHODS

Study design

Female rats at 12 weeks of age were obtained from Harlan Sprague–Dawley (Indianapolis, IN, USA). These rats had been raised under identical housing and dietary environments by Harlan Sprague–Dawley. The rats, representing 11 inbred strains (n = 6–7 from each strain), included ACI, Brown Norway (BN), Buffalo (BUF), Copenhagen 2331 (COP), DA, Fischer 344 (F344), Lewis (LEW), Munich Wistar (MW), PVG, Wistar Furth (WF), and Wistar Kyoto (WKY). These strains represent all of the commonly used inbred rat strains available from Harlan Sprague–Dawley, excluding strains of rats that are spontaneously hypertensive. They were kept in the animal facility at Indiana University for 8 weeks after delivery, during which they were maintained in the same room and received the same diet and were weighed weekly. At 20 weeks of age, the animals were killed and their femora and lumbar spine were collected for bone densitometry, biomechanical evaluation, and geometry measurements as described in the following sections. All specimens were stored in a −20°C freezer during interim periods. All animal procedures were approved by the Animal Care and Use Committee of the Indiana University School of Medicine.

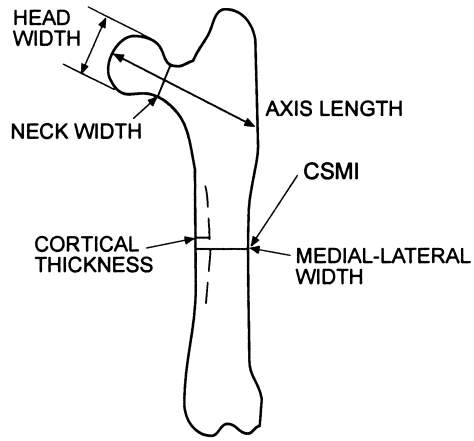

FIG. 1. Geometry measurements in the femur.

BMD measurement

The left hind leg and spinal column were dissected from the rats for BMD measurement of the left femur and lumbar vertebrae (L3–L5). BMD was measured using dual-energy X-ray absorptiometry (DXA) (Hologic QDR 1000/W; Hologic, Inc., Waltham, MA, USA) in regional high-resolution mode (0.70-mm beam collimator and 0.25-mm step size). All specimens were thawed before measurement and placed on a 1.5-in thick polyacrylic block used as a soft tissue equivalent during measurement. Measurements of projected area, bone mineral content (BMC), and areal BMD (aBMD) were recorded.

Bone geometry

Bone geometry measurements included the projected area of L3–L5 (from DXA), femoral length, cortical thickness at the midshaft of the femur, medial-lateral width of the midshaft of the femur, width of the femoral head, width of the femoral neck, and femoral neck axis length (Fig. 1). Femoral geometry measurements were made using digital calipers accurate to 0.005 mm. The value for the cross-sectional moment of inertia (CSMI) at the midshaft of the femur was calculated under the assumption that the femoral cross-sections were shaped elliptically. Previously, it has been shown that the elliptical cross-section model predicts the true CSMI within 5%.[14] The calculation of CSMI using the elliptical cross-section model is as follows:

$$\text{CSMI} = (\pi/64)[ab^3 - (a - 2t)(b - 2t)^3],$$

where a is the width of the cross-section in the mediolateral direction, b is the width of the bone in the anteroposterior direction, and t is the average cortical thickness. Average cortical thickness was calculated from thickness measurements made in each of the four quadrants of the femoral cross-section using digital calipers (cortical thickness measurements were made after biomechanical testing, i.e., after the femur was fractured).

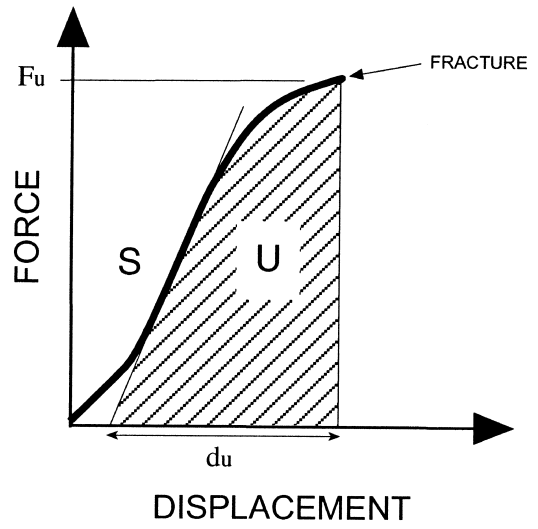

FIG. 2. Parameters derived from a biomechanical test. Ultimate force (F_u) represents the strength of the bone; ultimate displacement (d_u) is the ductility; the slope (S) represents bone stiffness; the work to failure (U) represents the energy the bone can absorb before it breaks.

Biomechanical tests

Biomechanical testing of a bone specimen produces several parameters that describe different aspects of bone fragility. These parameters are derived from the force-displacement curve (Fig. 2). Ultimate force (F_u) represents the strength of the bone; ultimate displacement (d_u) represents the ductility; the slope (S) represents bone stiffness; and the work to failure (U) represents the energy the bone can absorb before it breaks. Of these parameters, ultimate force is most commonly reported; however, work to failure is the parameter that may best describe bone fragility. Trauma imparts energy into the bone. If the traumatic energy exceeds the energy the bone can absorb (work to failure) the bone breaks. Thus, lower work to failure (area under the curve) may be caused either by decreased bone strength or by decreased ductility (i.e., decreased ultimate displacement).

Femur: Right femora were thawed before testing in three-point bending while submerged in a saline bath maintained at 37 ± 1°C. Load was applied midway between a 15-mm loading span at a crosshead speed of 20 mm/minute using a screw-driven mechanical testing machine (QTest IV; MTS Systems Corp., Eden Prairie, MN, USA). F_u, d_u, S, and U were determined from the load-displacement curve, which was stored in an ASCII file (Fig. 2). Intrinsic biomechanical properties were calculated using the following formulas:

$$\sigma_u = F_u\left(\frac{Lb}{8I}\right),$$

$$\varepsilon_u = d_u\left(\frac{6b}{L^2}\right),$$

$$E = S\left(\frac{L^3}{48I}\right), \quad \text{and}$$

$$u_T = U\left(\frac{3b^2}{4LI}\right),$$

where σ_u is ultimate stress, E is Young's modulus, u_T is modulus of toughness, ϵ_u is ultimate strain, L is the loading span (15 mm), b is the width of the femoral shaft in the anteroposterior direction, and I is the CSMI.[15]

Femoral neck: After the femoral three-point bending tests, the proximal one-half of each femur was mounted vertically in a special chuck that clamped the femoral shaft. Load was applied downward onto the femoral head at a rate of 20 mm/minute using a screw-driven mechanical testing machine (QTest IV) until the femoral neck fractured. F_u, d_u, S, and U were determined from the load-displacement curve.

Lumbar vertebra: L5 vertebrae were dissected from all soft tissues, and posterior elements were removed using small bone cutters. Specimens were clamped in an acrylic cutting fixture and parallel, transverse cuts were made at the end plates of the vertebral body using a diamond wafering saw (Isomet; Buehler, Lake Bluff, IL, USA). Specimens were thawed before testing in compression while submerged in a saline bath maintained at 37 ± 1°C. Load was applied at a crosshead speed of 20 mm/minute using a screw-driven mechanical testing machine (QTest IV). F_u, d_u, S, and U were determined from the load-displacement curve. Intrinsic biomechanical properties were calculated using the following formulas:

$$\sigma_u = \frac{F_u}{A},$$

$$\varepsilon_u = \frac{d_u}{h},$$

$$E = S\left(\frac{h}{A}\right), \quad \text{and}$$

$$u_T = \frac{U}{Ah},$$

where σ_u is ultimate stress, ϵ_u is ultimate strain, E is Young's modulus, u_T is modulus of toughness, h is the height of the sectioned vertebral body, and A is the cross-sectional area at the midcentrum.

Statistics

Analysis of variance (ANOVA) was used to compare the rat strains. Post hoc comparisons were performed using a Fisher's protected least significant difference test. The *t*-tests were used to compare the mean of each phenotype for each strain with the median values taken for all 11 strains. Simple regression analysis was used to compare measurements from different anatomical sites.

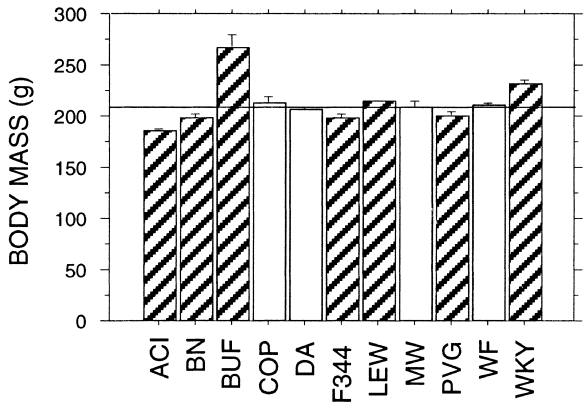

FIG. 3. Body mass for inbred strains of rats (error bars represent SEM). The horizontal line represents the median (208 g). The striped bars are significantly different from the median ($p < 0.05$).

RESULTS

Body mass varied among the strains ($p < 0.0001$; Fig. 3); BUF and WKY were significantly heavier than other strains ($p < 0.01$), and ACI was significantly lighter than the other strains ($p < 0.05$). In addition, femoral length varied significantly among the strains ($p < 0.0001$; Table 1). F344 rats had the shortest femoral length, which was significantly shorter than all other strains except BN, PVG, WF, and COP had the longest femora; femora from these strains were significantly longer than all other strains except BUF.

There were statistically significant differences ($p < 0.001$) among the strains of rats for all phenotypic variables presented in Table 1. The biomechanical integrity of the femur was well represented by the work to failure. F344 rats had the lowest femoral work to failure, whereas highest femoral work to failure was observed for DA rats (Fig. 4). The improved femoral work to failure in DA rats over F344 rats seemed to be caused by a larger than average femoral CSMI ($p < 0.05$). Femoral work to failure also was high in WF rats, apparently because of a greater than average cortical thickness. In addition, both DA and WF rats had high values of femoral modulus of toughness, a tissue level measure of resistance to fracture, suggesting that these strains not only had better femoral geometry, but also better bone quality. F344 rats had the lowest femoral modulus of toughness, suggesting more fragile femoral tissue. Although F344 and DA rats were similar in body size, the DA femur was significantly larger with greater bone mass. The DA rats had 13% greater femoral aBMD and 33% greater femoral CSMI compared with F344 rats. DA rats also had higher ultimate force (18%), ultimate displacement (41%), and work to failure (58%). In contrast, the ultimate stress and Young's modulus for the DA rats were significantly less than those for F344 rats, whereas the ultimate strain and toughness were much greater in the DA rats, suggesting that the femora from DA rats were less mineralized than the femora from F344 rats, and therefore less brittle.

COP rats clearly had superior work to failure of the femoral neck, while ACI rats had the most fragile femoral neck (Fig. 5). DA and WF rats also had more fragile femoral necks. The better femoral neck biomechanics in COP rats was caused by the combination of a thicker femoral neck and a shorter femur axis length. Compared with the ACI strain, the femoral neck from COP rats was significantly stronger (47% greater F_u), more ductile (188% greater d_u), and less fragile (338% greater U).

BUF rats had the greatest work to failure of lumbar vertebrae, while BN, F344, and MW rats had significantly more fragile vertebrae (Fig. 6). The improved vertebral biomechanics of BUF rats was caused by increased bone mass as well as larger vertebral bodies, which might reflect the substantially larger body size of BUF rats. Among the strains of rats with similar body size, LEW had high vertebral work to failure, BMC, and projected spine area while F344 and BN rats had fragile vertebrae with significantly reduced vertebral BMC and smaller vertebral bodies. The lowest vertebral work to failure was observed in the BN rats.

Biomechanical properties were not well correlated among the anatomical sites. For instance, work to failure U for the femoral midshaft was only weakly correlated with vertebral U ($r = 0.28$; $p < 0.05$), and femoral neck U was not correlated with femoral U ($p = 0.22$) or vertebral U ($p = 0.99$). These findings indicate that genetic control of biomechanical properties varies with anatomical site. In contrast, the bone mineral measurements were highly correlated: $r = 0.75$ for spine BMC versus femoral BMC and $r = 0.80$ for spine aBMD versus femoral aBMD.

DISCUSSION

It is widely recognized that age-related loss of aBMD is accompanied by increased risk of fracture.[16] In addition, certain aspects of skeletal geometry and structure are associated with fracture risk.[17,18] The results of this study show that considerable variation exists in bone geometry, bone mineral, and fragility phenotypes among inbred strains of rats. Thus, genetic studies in rats may uncover genes associated with skeletal fragility conditions in humans. The variability in skeletal biomechanical phenotypes in rats was site specific, suggesting that no single gene or group of genes regulate skeletal fragility at all clinically relevant sites; for example, genetic regulation of hip fragility might be somewhat independent of genetic effects on spine fragility. Interestingly, the variation in BMC and aBMD had little site specificity. Our findings suggest that mainly genetic regulation of bone geometry not BMC or aBMD causes the site-specific distribution of biomechanical properties. The variation found in our geometric measurements supports this conclusion. These data show that selected crosses of inbred strains of rats will provide useful models for studying genetic influences on bone strength and structure.

The data suggest complex genetic regulation of skeletal fragility. In many cases, rat strains had high bone strength at one skeletal site but only modest bone strength at others. An example is the COP strain, which had only modest bone strength at the femoral midshaft but high biomechanical

TABLE 1. PHENOTYPIC DATA FOR INBRED RAT STRAINS (MEAN ± SEM)

Measurement	*ACI*	*BN*	*BUF*	*COP*	*DA*	*F344*	*LEW*	*MW*	*PVG*	*WF*	*WKY*
Biomechanics											
Femur											
F_u (N)	94 ± 2	124 ± 5	132 ± 6	102 ± 4	114 ± 2	94 ± 4	110 ± 3	121 ± 5	126 ± 4	115 ± 1	110 ± 2
d_u (mm)	0.615 ± 0.022	0.550 ± 0.042	0.561 ± 0.033	0.477 ± 0.030	0.645 ± 0.031	0.380 ± 0.025	0.537 ± 0.025	0.537 ± 0.027	0.497 ± 0.013	0.632 ± 0.029	0.608 ± 0.034
S (N/mm)	309 ± 20	372 ± 5	404 ± 12	365 ± 16	337 ± 11	332 ± 15	351 ± 22	372 ± 13	430 ± 14	336 ± 12	334 ± 11
U (mJ)	40.4 ± 3.0	47.0 ± 4.7	49.9 ± 6.5	32.8 ± 2.8	52.3 ± 3.6	22.0 ± 2.6	39.4 ± 2.4	42.3 ± 3.2	41.3 ± 2.2	50.4 ± 2.7	47.0 ± 3.3
σ_u (MPa)	172 ± 2	209 ± 4	173 ± 6	200 ± 4	175 ± 5	200 ± 6	202 ± 5	184 ± 6	215 ± 3	207 ± 5	218 ± 6
ε_u (%)	4.20 ± 0.18	3.94 ± 0.26	4.15 ± 0.42	3.08 ± 0.20	4.85 ± 0.28	2.68 ± 0.18	3.63 ± 0.15	4.03 ± 0.25	3.56 ± 0.12	4.13 ± 0.20	4.02 ± 0.22
E (GPa)	8.3 ± 0.4	9.0 ± 0.3	7.2 ± 0.6	11.2 ± 0.5	6.9 ± 0.4	10.1 ± 0.5	9.5 ± 0.5	7.6 ± 0.4	10.3 ± 0.5	9.3 ± 0.5	10.1 ± 0.3
u_T (MJ/m^3)	5.05 ± 0.33	5.50 ± 0.50	4.78 ± 0.41	4.15 ± 0.33	6.06 ± 0.47	3.27 ± 0.28	4.91 ± 0.33	4.79 ± 0.31	5.02 ± 0.22	5.92 ± 0.38	6.21 ± 0.52
Femoral Neck											
F_u (N)	68.5 ± 2.1	69.1 ± 1.1	102.2 ± 5.5	100.5 ± 9.0	70.6 ± 4.6	86.9 ± 1.9	94.9 ± 3.3	74.3 ± 3.9	78.7 ± 1.9	76.9 ± 3.7	80.5 ± 1.1
d_u (mm)	0.253 ± 0.028	0.349 ± 0.025	0.332 ± 0.021	0.730 ± 0.094	0.334 ± 0.044	0.487 ± 0.070	0.287 ± 0.029	0.411 ± 0.051	0.340 ± 0.024	0.290 ± 0.030	0.405 ± 0.042
S (N/mm)	357 ± 11	274 ± 9	369 ± 16	224 ± 10	276 ± 6	267 ± 44	459 ± 21	291 ± 12	315 ± 13	370 ± 8	287 ± 16
U (mJ)	10.3 ± 1.9	14.4 ± 1.4	19.1 ± 2.6	45.1 ± 9.3	13.4 ± 2.6	24.4 ± 3.3	16.4 ± 2.1	20.5 ± 4.4	15.7 ± 1.6	13.8 ± 2.7	19.0 ± 2.3
Vertebra (L5)											
F_u (N)	273 ± 18	198 ± 25	451 ± 42	300 ± 17	280 ± 13	222 ± 25	330 ± 34	220 ± 14	252 ± 32	308 ± 25	306 ± 21
d_u (mm)	0.373 ± 0.061	0.257 ± 0.030	0.237 ± 0.037	0.252 ± 0.037	0.372 ± 0.044	0.285 ± 0.032	0.270 ± 0.039	0.300 ± 0.028	0.278 ± 0.046	0.228 ± 0.025	0.260 ± 0.033
S (N/mm)	1191 ± 106	884 ± 96	2373 ± 369	1260 ± 184	1083 ± 141	1005 ± 166	1590 ± 241	1039 ± 69	1003 ± 86	1707 ± 190	1417 ± 234
U (mJ)	67.2 ± 7.5	35.1 ± 7.3	78.4 ± 12.0	58.8 ± 2.9	65.8 ± 5.3	36.8 ± 4.7	62.6 ± 6.9	40.5 ± 4.8	48.1 ± 9.5	48.8 ± 2.8	52.5 ± 3.5
σ_u (MPa)	29.9 ± 2.1	22.9 ± 3.2	46.0 ± 3.2	32.8 ± 1.8	32.6 ± 2.0	35.3 ± 2.3	41.6 ± 3.3	28.3 ± 1.4	40.2 ± 4.6	37.5 ± 3.2	36.5 ± 3.0
ε_u (%)	15.6 ± 2.6	9.9 ± 1.3	9.8 ± 1.4	9.2 ± 1.2	15.2 ± 1.9	12.4 ± 1.1	12.6 ± 1.6	12.7 ± 1.1	10.5 ± 1.6	10.3 ± 1.1	10.7 ± 1.3
E (MPa)	312 ± 28	270 ± 39	571 ± 73	367 ± 47	312 ± 47	359 ± 51	413 ± 36	322 ± 32	425 ± 51	456 ± 43	412 ± 71
u_T (MJ/m^3)	3.07 ± 0.38	1.59 ± 0.37	3.34 ± 0.43	2.38 ± 0.08	3.10 ± 0.25	2.57 ± 0.21	3.78 ± 0.44	2.17 ± 0.17	2.90 ± 0.48	2.70 ± 0.22	2.55 ± 0.12
Bone density											
Femur											
BMC (g)	0.339 ± 0.007	0.328 ± 0.005	0.425 ± 0.014	0.384 ± 0.011	0.351 ± 0.004	0.280 ± 0.006	0.354 ± 0.006	0.339 ± 0.009	0.386 ± 0.008	0.360 ± 0.006	0.324 ± 0.002
aBMD (g/cm^2)	0.253 ± 0.003	0.250 ± 0.003	0.307 ± 0.004	0.271 ± 0.004	0.263 ± 0.002	0.228 ± 0.003	0.266 ± 0.003	0.256 ± 0.002	0.267 ± 0.003	0.268 ± 0.003	0.251 ± 0.002
Vertebrae (L2–L5)											
BMC (g)	0.269 ± 0.013	0.276 ± 0.008	0.428 ± 0.026	0.337 ± 0.014	0.291 ± 0.008	0.240 ± 0.011	0.341 ± 0.007	0.293 ± 0.013	0.314 ± 0.013	0.341 ± 0.011	0.307 ± 0.014
aBMD (g/cm^2)	0.218 ± 0.003	0.206 ± 0.004	0.257 ± 0.006	0.228 ± 0.004	0.224 ± 0.002	0.202 ± 0.004	0.230 ± 0.003	0.211 ± 0.004	0.225 ± 0.005	0.225 ± 0.005	0.211 ± 0.005
Geometry											
Femur											
Length (mm)	33.0 ± 0.12	32.3 ± 0.11	33.4 ± 0.36	33.7 ± 0.14	33.0 ± 0.10	31.8 ± 0.19	33.0 ± 0.09	32.6 ± 0.28	33.9 ± 0.13	33.8 ± 0.26	32.6 ± 0.16
Cortical thickness (mm)	0.67 ± 0.02	0.67 ± 0.02	0.71 ± 0.02	0.71 ± 0.01	0.64 ± 0.01	0.66 ± 0.02	0.76 ± 0.01	0.64 ± 0.02	0.66 ± 0.01	0.74 ± 0.02	0.65 ± 0.02
M-L width (mm)	3.48 ± 0.05	3.32 ± 0.04	3.93 ± 0.10	3.52 ± 0.04	3.59 ± 0.04	2.84 ± 0.04	3.38 ± 0.04	3.34 ± 0.10	3.36 ± 0.07	3.55 ± 0.03	3.33 ± 0.01
Head width (mm)	3.77 ± 0.04	3.65 ± 0.03	3.77 ± 0.03	3.77 ± 0.04	3.61 ± 0.01	3.68 ± 0.02	3.54 ± 0.01	3.67 ± 0.03	3.64 ± 0.03	3.52 ± 0.03	3.83 ± 0.02
Neck width (mm)	2.58 ± 0.04	2.43 ± 0.03	2.73 ± 0.13	2.75 ± 0.05	2.46 ± 0.05	2.46 ± 0.06	2.40 ± 0.04	2.40 ± 0.06	2.47 ± 0.02	2.54 ± 0.02	2.40 ± 0.01
Axis length (mm)	9.05 ± 0.13	8.43 ± 0.11	9.01 ± 0.14	8.52 ± 0.11	8.82 ± 0.15	8.97 ± 0.08	8.77 ± 0.12	8.91 ± 0.15	8.58 ± 0.08	8.97 ± 0.09	9.28 ± 0.08
CSMI (mm^4)	2.61 ± 0.08	2.93 ± 0.12	4.09 ± 0.42	2.31 ± 0.08	3.44 ± 0.14	2.32 ± 0.08	2.61 ± 0.08	3.50 ± 0.24	2.97 ± 0.14	2.57 ± 0.08	2.35 ± 0.12
Vertebrae (L3–L5)											
Projected area (cm^2)	1.23 ± 0.05	1.34 ± 0.02	1.66 ± 0.07	1.48 ± 0.04	1.30 ± 0.03	1.19 ± 0.04	1.48 ± 0.02	1.38 ± 0.04	1.39 ± 0.03	1.51 ± 0.03	1.45 ± 0.03
Body mass (g)	185 ± 2	199 ± 3	266 ± 12	214 ± 5	207 ± 2	199 ± 2	214 ± 2	208 ± 6	200 ± 3	211 ± 2	231 ± 3

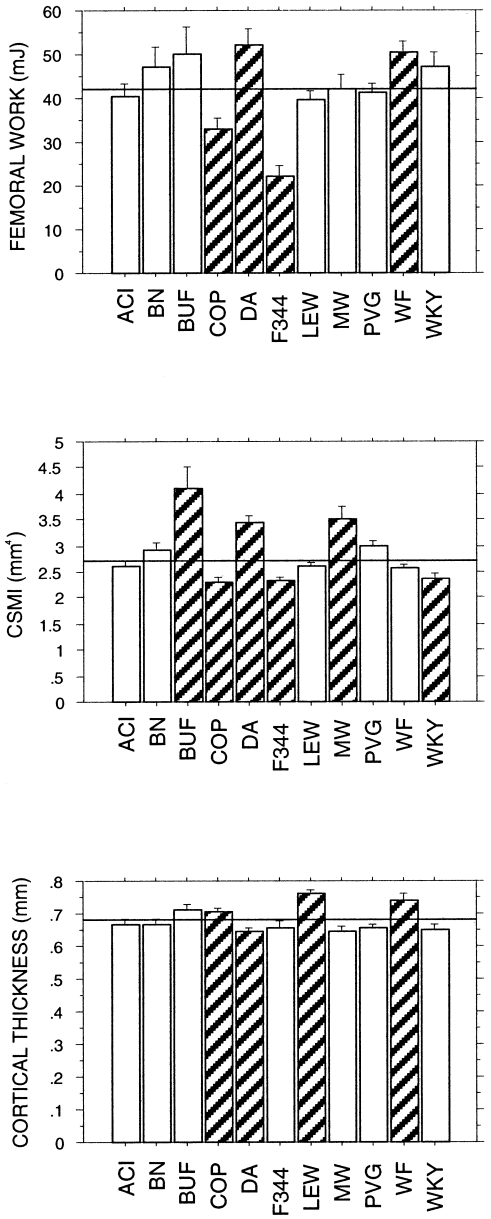

FIG. 4. Femoral work to failure, CSMI at the femoral midshaft, and femoral cortical thickness for inbred strains of rats (error bars represent SEM). The horizontal lines represent the median values: 42.3 mJ for work, 2.72 mm^4 for CSMI, and 0.68 mm for cortical thickness. The striped bars are significantly different from the median ($p < 0.05$).

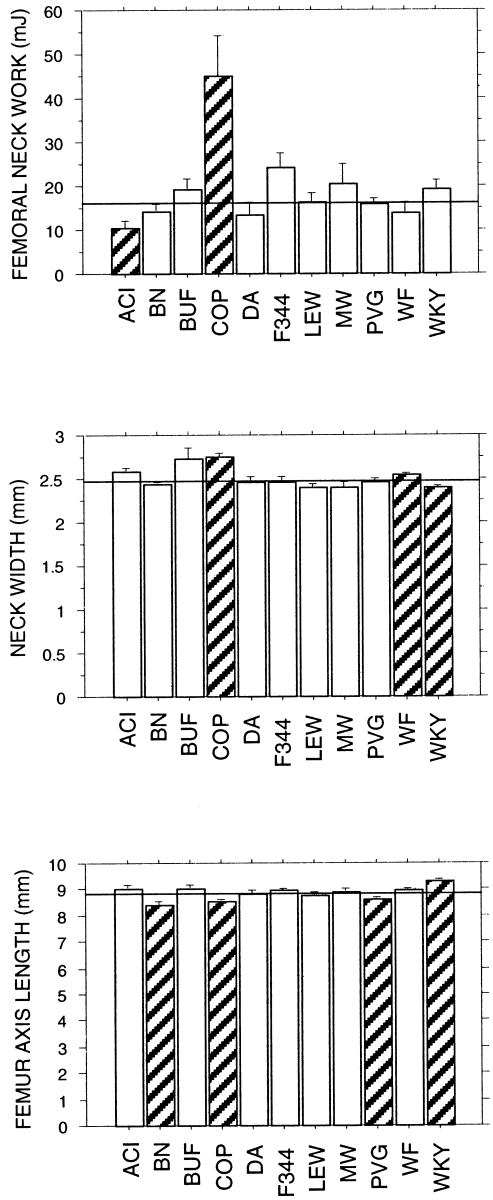

FIG. 5. Work to failure and geometric measurements for the femoral neck of inbred strains of rats (error bars represent SEM). The horizontal lines represent the median values: 16.3 mJ for work, 2.48 mm for neck width, and 8.86 mm for femur axis length. The striped bars are significantly different from the median ($p < 0.05$).

properties in the femoral neck, compared with other strains. The latter was associated with a thicker and shorter femoral neck. Consequently, COP rats appear to have alleles that specifically enhance femoral neck structure and biomechanical properties offering a compelling model for the study of hip fragility. Similarly, the BN and F344 strains may provide models for vertebral fragility because each have relatively fragile lumbar vertebrae. The F344 rats had the most fragile femora, and thus appear to carry alleles that cause overall skeletal fragility.

One approach for identifying the genetic loci regulating a skeletal phenotype involves the creation and genetic mapping of a population of F2 offspring derived from a cross of two inbred strains.[19] The two inbred strains (i.e., the grandparents of the F2 offspring) should be chosen based on a large difference in the phenotype of interest but matched for body size and weight and other factors known to be related to bone strength and structure. From the data collected in this study it is possible to identify inbred rat crosses that will facilitate the study of genetic influences on skeletal fragility at the skeletal sites investigated. The two most compelling crosses are LEW with F344 (LEW × F344, primarily for

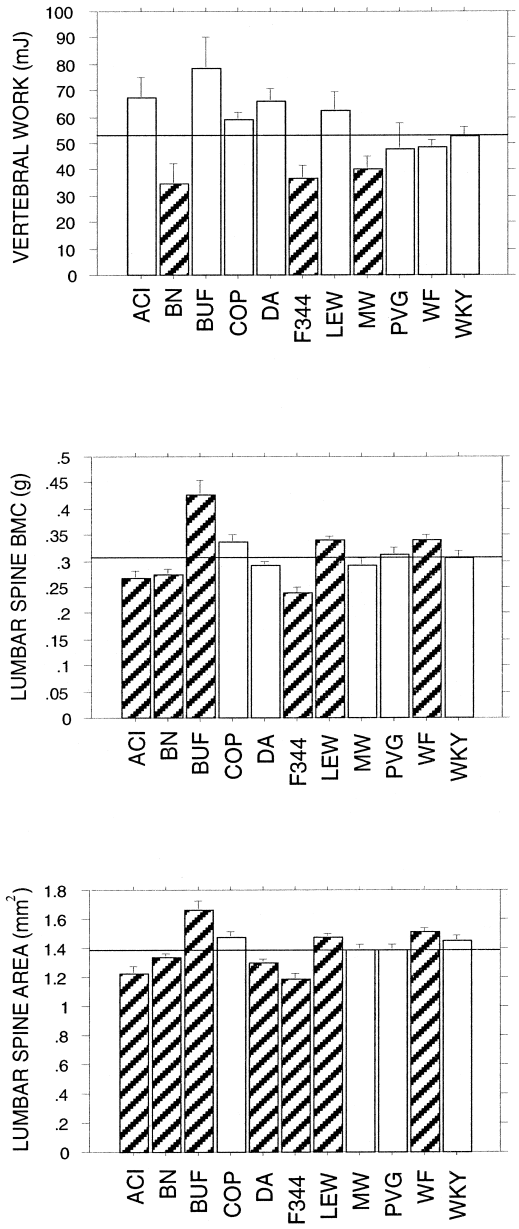

FIG. 6. Work to failure, BMC, and geometry for the lumbar vertebrae of inbred strains of rats (error bars represent SEM). The horizontal lines represent the median values: 52.9 mJ for work, 0.309 g for BMC, and 1.39 mm^2 for projected area of the lumbar spine (L3–L5). The striped bars are significantly different from the median ($p < 0.05$).

vertebral fragility) and COP with DA (COP × DA, primarily for femoral neck fragility). COP and DA rats showed the most variation in femoral neck biomechanical properties (if one eliminates the ACI strain because of their significantly smaller body size). Femoral neck work to failure for COP was over 3-fold greater than DA. In addition, the femoral neck was significantly wider and shorter in COP. LEW and F344 strains showed the greatest phenotypic variation at the lumbar spine (if one eliminates the BUF strain because of their much larger body size). Moreover, both crosses show significant variation in the femoral shaft phenotype. LEW and F344 have large differences in work to failure of the femoral midshaft and cortical thickness, while COP and DA are different mainly in the CSMI of the femoral midshaft, which results in a difference in femoral work to failure.

For this study, we chose 20-week-old female rats, which equate with young women. Our aim was to choose animals with peak bone strength. Genes that influence the attainment of peak bone strength or density also should protect against osteoporosis in later years. In women, high peak bone density is associated with lower risk of osteoporosis.[20] Previous studies using female Sprague–Dawley rats show a decline in femoral midshaft and neck strength beginning at or before 27 weeks of age (C.H. Turner, unpublished data, 1995).[21] Vertebral trabecular bone volume began to decline as early as 15 weeks.[21] From these data we concluded that peak bone mass and bone strength occurred within a window of 15–27 weeks of age in rats; hence, our choice of 20-week-old rats. Others suggest that rats achieve peak bone density between 24 and 36 weeks of age.[22] It is not established that skeletal growth in inbred strains of rats resembles that shown for the outbred Sprague–Dawley strain. We cannot exclude the possibility that the inbred strains we studied develop bone strength and density at different rates and that this variability in growth contributed to a portion of the variation in phenotypes we observed.

We conclude that considerable variability exists among inbred strains of rats for skeletal phenotypes. However, the phenotypic variation is site specific. Two crosses of rat strains, LEW × F344 and COP × DA, will facilitate studies of genetic loci influencing skeletal structure and fragility at the femoral neck, lumbar spine, and femoral midshaft and will complement ongoing human studies focused on identifying genetic loci influencing aBMD. Unlike human studies, controlled breeding studies in rats allow direct measurement of bone fragility and thus extend our knowledge of the genetics of osteoporosis beyond genetic influences on aBMD. In addition, rats offer some advantages over mice for genetic studies. Because of the small size of mouse bones, biomechanical measurements, particularly vertebral compressive tests, have greater variability compared with tests using rat bones. For instance, the CV for vertebral *U* measured previously by our laboratory for C57BL/6J mice[23] was about twice that for the rats in this study. BMD measurements in mice are more sensitive to partial volume averaging errors than are measurements in rats, again because of the small size of mouse bones, and bone geometry measurements are made more easily in rats. Finally, the femoral neck strength phenotype found in COP rats provides a model for genetic effects on hip strength not currently available in mice.

ACKNOWLEDGMENTS

This work was supported in part by the U.S. Public Health Service National Institutes of Health grants AR43730 (C.H.T.), AG13408 (M.P.), and P01AG18397.

REFERENCES

1. Pocock NA, Eisman JA, Hopper JL, Yeates MG, Sambrook PN, Eberl S 1987 Genetic determinants of bone mass in adults: A twin study. J Clin Invest **80:**706–710.
2. Slemenda CW, Christian JC, Williams CJ, Norton JA, Johnston CC 1991 Genetic determinants of bone mass in adult women: A reevaluation of the twin model and the potential importance of gene interaction on heritability estimates. J Bone Miner Res **6:**561–567.
3. Smith DM, Nance WE, Kang KW, Christian JC, Johnston CC Jr 1973 Genetic factors in determining bone mass. J Clin Invest **52:**2800–2808.
4. Foroud T, Li T-K 1999 Genetics of alcoholism: A review of recent studies in human and animal models. Am J Addict **8:**261–278.
5. Beamer WG, Rosen CJ, Donahue LR, Frankel WN, Churchill GA, Shultz KL, Baylink DJ 1998 Location of genes regulating volumetric bone mineral density in C57BL/6J (low) and C3H/HeJ (high) inbred strains of mice (abstract). Bone **23**(Suppl)**:** S162.
6. Klein RF, Mitchell SR, Phillips TJ, Belknap JK, Orwoll ES 1998 Quantitative trait loci affecting peak bone mineral density in mice. J Bone Miner Res **13:**1648–1656.
7. Wronski TJ, Dann LM, Horner SL 1989 Time course of vertebral osteopenia in ovariectomized rats. Bone **10:**295–301.
8. Wronski TJ, Cintron M, Dann LM 1988 Temporal relationship between bone loss and increased bone turnover in ovariectomized rats. Calcif Tissue Int **43:**179–183.
9. Bonjour JP, Ammann P, Rizzoli R 1999 Importance of preclinical studies in the development of drugs for treatment of osteoporosis: A review related to the 1998 WHO guidelines. Osteoporos Int **9:**379–393.
10. RATMAP at http://ratmap.gen.gu.se/.
11. Steen RG, Kwitek-Black AE, Glenn C, Gullings-Handley J, Van Etten W, Atkinson OS, Appel D, Twigger S, Muir M, Mull T, Granados M, Kissebah M, Russo K, Crane R, Popp M, Peden M, Matise T, Brown DM, Lu J, Kingsmore S, Tonellato PJ, Rozen S, Slonim D, Young P, Jacob HJ 1999 A high-density integrated genetic linkage and radiation hybrid map of the laboratory rat. Genome Res **9:**AP1–8 (insert).
12. Watanabe TK, Bihoreau MT, McCarthy LC, Kiguwa SL, Hishigaki H, Tsuji A, Browne J, Yamasaki Y, Mizoguchi-Miyakita A, Oga K, Ono T, Okuno S, Kanemoto N, Takahashi E, Tomita K, Hayashi H, Adachi M, Webber C, Davis M, Kiel S, Knights C, Smith A, Critcher R, Miller J, James MR 1999 A radiation hybrid map of the rat genome containing 5,255 markers. Nat Genet **22:**27–36.
13. Dracheva SV, Remmers EF, Chen S, Chang L, Gulko PS, Kawahito Y, Longman RE, Wang J, Du Y, Shepard J, Ge L, Joe B, Kotake S, Salstrom JL, Furuya T, Hoffman J, Cannon GW, Griffiths MM, Wilder RL 2000 An integrated genetic linkage map with 1137 markers constructed from five F2 crosses of autoimmune disease-prone and -resistant inbred rat strains. Genomics **63:**202–226.
14. Keller TS, Spengler DM, Carter DR 1986 Geometric, elastic, and structural properties of maturing rat femora. J Orthop Res **4:**57–67.
15. Turner CH, Burr DB 1993 Basic biomechanical measurements of bone: A tutorial. Bone **14:**595–608.
16. Cummings SR, Black DM, Nevitt MC, Browner W, Cauley J, Ensrud K, Genant HK, Palermo L, Scott J, Vogt TM 1993 Bone density at various sites for prediction of hip fractures. The Study of Osteoporotic Fractures Research Group. Lancet **341:**72–75.
17. Peacock M, Turner CH, Liu G, Manatunga AK, Timmerman L, Johnston CC Jr 1995 Better discrimination of hip fracture using bone density, geometry and architecture. Osteoporos Int **5:**167–173.
18. Faulkner KG, Cummings SR, Black D, Palermo L, Gluer CC, Genant HK 1993 Simple measurement of femoral geometry predicts hip fracture: The study of osteoporotic fractures. J Bone Miner Res **8:**1211–1217.
19. Beamer WG, Shultz KL, Churchill GA, Frankel WN, Baylink DJ, Rosen CJ, Donahue LR 1999 Quantitative trait loci for bone density in C57BL/6J and CAST/EiJ inbred mice. Mamm Genome **10:**1043–1049.
20. Riis BJ, Hansen MA, Jensen AM, Overgaard K, Christiansen C 1996 Low bone mass and fast rate of bone loss at menopause: Equal risk factors for future fracture: A 15-year follow-up study. Bone **19:**9–12.
21. Turner CH, Hasegawa K, Zhang W, Wilson M, Li Y, Dunipace AJ 1995 Fluoride reduces bone strength in older rats. J Dent Res **74:**1475–1481.
22. Frost HM, Jee WSS 1992 On the rat model of human osteopenias and osteoporoses. Bone Miner **18:**227–236.
23. Turner CH, Hsieh Y-F, Müller R, Bouxsein ML, Baylink DJ, Rosen CJ, Grynpas MD, Donahue LR, Beamer WG 2000 Genetic regulation of cortical and trabecular bone strength and microstructure in inbred strains of mice. J Bone Miner Res **15:**1126–1131.

Address reprint requests to:
Charles H. Turner, Ph.D.
Director of Orthopedic Research
541 Clinical Drive, Room 600
Indianapolis, IN 46202, USA

Received in original form March 28, 2000; in revised form August 2, 2000; accepted November 7, 2000.